Atomic Positional Versus Electronic Order in Semiconducting ZnSe Nanoparticles

S. Cadars,[1] B. J. Smith,[1] J. D. Epping,[1] S. Acharya,[2] N. Belman,[2] Y. Golan,[2] and B. F. Chmelka[1,*]

[1]*Department of Chemical Engineering, University of California, Santa Barbara, California 93106, USA*

[2]*Department of Materials Engineering, Ben-Gurion University, Beer-Sheva 84105, Israel*

(Received 18 February 2009; published 24 September 2009)

Size-controlled ZnSe nanoparticles with high extents of atomic positional order are shown to exhibit large size-dependent variations in their local electronic environments. Solid-state ^{77}Se and ^{67}Zn NMR spectra reveal increasingly broad distributions of ^{77}Se and ^{67}Zn environments with decreasing nanoparticle sizes, in contrast with high degrees of atomic positional order established by transmission electron microscopy and x-ray diffraction. First-principles calculations of NMR parameters distinguish between atomic positional and electronic disorder that propagate from the nanoparticle surfaces and yield insights on the order and disorder present.

DOI: 10.1103/PhysRevLett.103.136802 PACS numbers: 73.22.−f, 71.15.Mb, 73.61.Ga, 82.56.−b

Nanoparticles have been the focus of intense research interest because their size-dependent properties are generally different from bulk materials with similar compositions [1–3]. Recent advances in syntheses of nanoparticles allow their sizes, shapes, morphologies, and compositions to be controlled within narrow distributions [4,5] that have enabled fundamental studies and comparisons of their physicochemical properties [6,7]. In particular, numerous semiconducting compounds and metals have been prepared with high degrees of local atomic positional order, as evidenced by scattering and electron microscopy measurements [8,9], which have led to their designation as ''nanocrystals.'' Resulting applications benefit from more uniform macroscopic properties that are not complicated by otherwise broad distributions of nanoparticle sizes, shapes, and/or atomic disorder.

Nevertheless, even for uniform particles, nanoscale dimensions inherently lead to large surface areas that can contribute importantly to nanoparticle properties. Abrupt discontinuities at nanoparticle surfaces generally exert large influences on surface compositions and bonding [10]. The extent to which such surface influences penetrate into the interiors of nanoparticles, however, is largely unknown. This is due, in part, to challenges in characterizing heterogeneities in nanoscale materials, which inherently lack long-range, and often even short-range, molecular order.

Here, the extents of atomic positional order and local electronic order within the internal structures of semiconducting nanoparticles are distinguished and shown to differ. ZnSe nanoparticles are used as an example, the sizes and shapes of which were controlled by syntheses in the presence of varying ratios of octadecylamine (ODA) and trioctylphosphineoxide (TOPO) surfactant species (Ref. [11], Fig. S1). Different ODA:TOPO molar ratios yield ZnSe nanoparticles ([11], Fig. S2) with different adjustable and relatively uniform shapes and sizes [5], as shown in the representative TEM images of Figs. 1(a)–1(c). All of the nanoparticles observed exhibit well-defined lattice fringes, associated with scattering from ordered core electrons that manifest high extents of atomic positional order. Faceted ZnSe spheroids with a mean diameter of 9 nm (standard deviation, SD 2 nm) were obtained from a 1:1 molar mixture of ODA:TOPO [Fig. 1(a)]. Prolate nanorods with a mean diameter of 5 nm (SD 2 nm) [Fig. 1(b)] were predominantly formed using only TOPO surfactant species, while ultranarrow nanorods 1.3 nm (SD 0.4 nm) in diameter [Fig. 1(c)] were synthesized using only ODA. Powder XRD patterns show wide-angle reflections that are indexable to the expected bulk cubic zinc blende (ZB) structure for the 9- and 5-nm ZnSe nanoparticles [Fig. 1(d)]. By comparison, the ODA-capped 1.3-nm ZnSe nanorods exhibit reflections

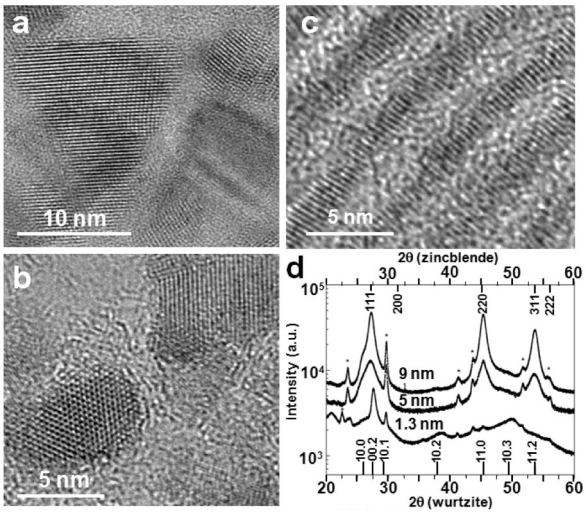

FIG. 1. (a)–(c) Representative high-resolution TEM images of ZnSe nanoparticles with different mean sizes: (a) 9, (b) 5, and (c) 1.3 nm, and (d) the corresponding powder XRD patterns of the same samples. The * symbols indicate reflections assigned to surfactant species.

that are indexable to a hexagonal wurtzite (WZ) structure [Fig. 1(d)], which is not typically associated with bulk ZnSe [5,12]. The XRD patterns are consistent with the well-defined lattice fringes observed in the TEM images in Figs. 1(a)–1(c), indicating high extents of positional order of Se and Zn atoms in these ZnSe nanoparticles, within the resolution limits of the scattering measurements [13].

In contrast, solid-state ^{77}Se and ^{67}Zn magic-angle spinning (MAS) NMR measurements [11] of the same ZnSe nanoparticle samples show very different extents of local electronic order, in spite of their apparently high extents of atomic positional order. The NMR signals of ^{77}Se (spin $I = 1/2$, 7.6% nat. abund.) and ^{67}Zn (spin $I = 5/2$, 4.1% nat. abund.) are sensitive to their local environments. Solid-state ^{77}Se NMR has previously been used to characterize surface and local structures of chalcogenides [14], including nanoparticles [15,16]. By comparison, there have been far fewer studies of inorganic materials using solid-state ^{67}Zn NMR [14,17,18], due in part to the low gyromagnetic ratio, low natural abundance, and the quadrupolar character of ^{67}Zn, which result in low signal sensitivity and poor spectral resolution, which are both significantly improved at very high magnetic fields.

Bulk polycrystalline ZnSe is predominantly comprised of Zn and Se sites with high degrees of both atomic positional and electronic order. Sharp wide-angle XRD reflections ([11], Fig. S3) establish the cubic zinc blende structure, with long-range positional ordering of single crystallographically distinct Zn and Se sites within bulk (ca. 5 μm) ZnSe particles. This atomic positional ordering is accompanied by high degrees of electronic order, as manifested by the narrow ^{77}Se and ^{67}Zn NMR signals (ca. 1 and 3 ppm fwhm, respectively) at −351 and 275 ppm shown in Figs. 2(a) and 2(e).

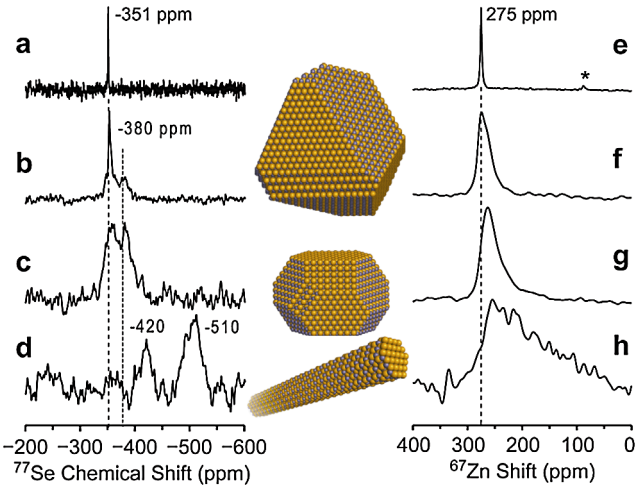

FIG. 2 (color online). Solid-state (a)–(d) single-pulse ^{77}Se (11.7 T) and (e)–(h) spin-echo ^{67}Zn (19.6 T) MAS NMR spectra of (a),(e) bulk ZnSe, and the same ZnSe nanoparticle samples in Fig. 1 with mean diameters: (b),(f) 9, (c),(g) 5, and (d),(h) 1.3 nm.

By comparison, for "nanocrystalline" ZnSe particles with sizes below ca. 10 nm, solid-state MAS NMR spectra reveal much broader distributions of local electronic environments around otherwise predominantly positionally ordered ^{77}Se and ^{67}Zn sites. For the same 9, 5, and 1.3 nm diameter ZnSe nanoparticle samples shown in Fig. 1, the ^{77}Se MAS spectra [Figs. 2(b)–2(d)] exhibit much broader linewidths, manifesting large chemical shift dispersions, compared to bulk polycrystalline ZnSe [Fig. 2(a)]. In Fig. 2(b), for the 9-nm ZnSe nanoparticles, a sharp (5 ppm fwhm) signal at −351 ppm is observed, consistent with an appreciable fraction of ^{77}Se atoms in approximately crystalline bulklike local environments. However, in addition, a significantly broader (ca. 35 ppm fwhm) component is present underlying the bulk peak and also broad upfield intensity at −380 ppm. For the 5-nm ZnSe nanoparticles [Fig. 2(c)], the narrow bulk peak is not visible, having been replaced entirely by the broad partially resolved signals at ca. −350 and −380 ppm, which increase in intensity as the nanoparticles become smaller. These broadened and displaced ^{77}Se signals correlate with the greater relative surface-to-volume fraction of the 5-nm ZnSe nanoparticles, compared to the 9-nm nanoparticles or polycrystalline ZnSe.

The appearance of significantly broader ^{77}Se MAS NMR signals for ZnSe nanoparticles with mean diameters smaller than ca. 10 nm reflects larger contributions from distributions of local environments near the nanoparticle surfaces. The broadened and upfield-shifted ^{77}Se MAS signal intensities in Figs. 2(b) and 2(c) indicate that local nonbulk ^{77}Se environments near the ZnSe nanoparticle surfaces propagate toward their cores, despite the high degrees of atomic positional order revealed by TEM and XRD (Fig. 1). Based on the absence of a sharp bulklike ^{77}Se signal at −351 ppm for the 5-nm nanoparticles, the surface-induced perturbations of the electronic density at ^{77}Se sites persist ca. 2 nm from the ZnSe nanoparticle surfaces.

The ^{77}Se MAS spectrum of even smaller ZnSe nanoparticles is consistent with the large influence of surface effects on the electronic environments of interior ^{77}Se sites, although analyses are complicated by different atom configurations. Specifically, ultranarrow 1.3 nm nanorods [Fig. 2(d)] show broad ^{77}Se signals centered at −420 and −510 ppm, but no signal intensity corresponding to bulklike ZnSe environments (ca. −350 ppm). As discussed above, the 1.3-nm ZnSe nanoparticles have a hexagonal wurtzite (WZ) structure [5], so that the absence of a ^{77}Se signal at −351 ppm could be due to a difference in chemical shifts between ^{77}Se atoms in bulk ZB versus WZ environments. Although the bulk WZ ZnSe structure is not stable under ambient conditions and the corresponding ^{77}Se chemical shift(s) thus not experimentally measurable, they can nevertheless be calculated from first-principles. This permits differences in the bulk zinc blende and wurtzite structures to be quantitatively assessed independently

from surface-bonding effects (e.g., localized lattice contractions or expansions) at the nanoparticle surfaces.

Predictions of ^{77}Se NMR parameters were performed by using the plane-wave-based density functional theory (DFT) code CASTEP [19,20], where long-range solid-state environments are described through periodic boundary conditions. Calculations performed on bulk ZnSe systems with WZ and ZB structures predict that polycrystalline WZ ZnSe (if it existed) would yield a sharp ^{77}Se NMR resonance between −365 and −380 ppm. The clear absence of ^{77}Se signal intensity between −350 and −400 ppm for the 1.3-nm WZ ZnSe nanoparticles [Fig. 2(d)] thus indicates that surface-induced effects are predominantly responsible for the non-bulk-like electronic environments in these particles. Although TEM and XRD results establish a high degree of atomic positional order in these ultrasmall particles, the ^{77}Se NMR measurements and DFT analyses point to a much lower extent of overall electronic order.

^{67}Zn nuclei are similarly sensitive to local disorder in ZnSe nanoparticles, though the analyses are complicated by their quadrupolar nature. Figures 2(f)–2(h) show solid-state ^{67}Zn MAS NMR spectra of the same nanoparticle samples as in Figs. 1 and 2(b)–2(d), recorded at 19.6 T to provide enhanced sensitivity and resolution. The single narrow ^{67}Zn resonance at 275 ppm [Fig. 2(e)] from bulk polycrystalline ZnSe is consistent with ^{67}Zn atoms in symmetric cubic sites in the zinc blende structure. By comparison, the ^{67}Zn MAS spectra of ZnSe nanoparticles with mean diameters of 9, 5, and 1.3 nm [Figs. 2(f)–2(h)] show increasingly broad and upfield-shifted resonances that result from broader distributions of local ^{67}Zn environments and thus larger dispersions of ^{67}Zn shifts. Compared to the ^{77}Se spectra, the broader ^{67}Zn MAS linewidths are consistent with significant additional contributions from second-order quadrupolar interactions that result from the diminished symmetry of electric-field gradients at ^{67}Zn sites near the nanoparticle surfaces. The solid-state ^{67}Zn and ^{77}Se MAS NMR results, thus, directly and independently establish that increasingly large distributions of local electronic environments are present in ZnSe nanoparticles with decreasing sizes.

More specific insights on the nature and origin of the disorder observed by NMR are obtained from DFT calculations of ^{77}Se and ^{67}Zn chemical shifts [11]. Computations were conducted using ZnSe ZB supercells with two exposed charge-neutral (110) surfaces as representative for ZnSe nanoparticles, with surface-capping H_3PO molecules to approximate interactions with the TOPO surfactant head groups [21] (for the 5-nm particles.) After optimization of the H_3PO adsorption geometry [11], DFT calculations of ^{77}Se chemical shifts were conducted on systems containing various numbers of (110) layers to probe electronic and structural environments at different atomic distances from the exterior ZnSe nanoparticle surfaces.

Model systems with sufficiently large numbers of ZnSe layers permit detailed analyses of the effects that explain the experimental ^{77}Se NMR spectra of ZnSe nanoparticles at a molecular level. For example, Fig. 3 shows the ^{77}Se isotropic chemical shifts of sites at different distances from a ZnSe surface calculated using supercells containing 9 or 17 ZB (110) ZnSe layers. For 50% H_3PO coverage (energetically favored over higher surface concentrations), each ZnSe layer has two types of ^{77}Se atoms that are distinguished by their proximities to the adsorbed H_3PO molecules (Fig. 3, right). The calculations show that the broad ^{77}Se signal(s) in the range −380 to −420 ppm can be attributed to ^{77}Se atoms in the first two layers, whose resonances are shifted upfield relative to bulk environments, due to combined effects of surface relaxation (∼2–3%) and interactions with H_3PO molecules adsorbed on nearby surface Zn atoms.

By comparison, the chemical shifts of otherwise positionally ordered ^{77}Se atoms located farther below the surface are principally affected by surface-induced electronic perturbations. In our optimizations of the H_3PO adsorption geometry, whereas atomic positions were allowed to relax in the first two ZnSe layers, the atoms located farther from the surface were fixed to their bulk positions. Thus, the propagation of surface-induced electronic perturbations into the ZnSe particle interiors could be probed in the absence of atomic positional disorder and/or independently of small amplitude positional variations that may underlie the intrinsic Debye-Scherrer-broadened XRD reflections of nanoscale particles. Importantly, damped 20–70 ppm displacements of the calculated isotropic ^{77}Se shifts on both sides of the −351 ppm bulk signal are observed for ^{77}Se sites 0.2–1.2 nm from the exterior surface. These calculated ^{77}Se shifts are consistent with the broadening

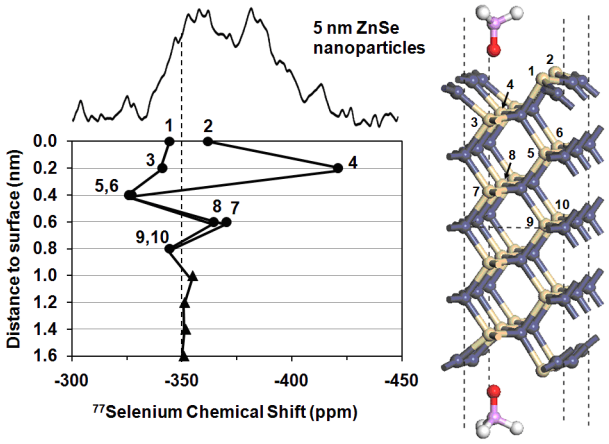

FIG. 3 (color online). Calculated isotropic ^{77}Se chemical shifts versus the distances of ^{77}Se atoms from the nearest surface of a 9-layer ZnSe ZB supercell (right) with two exposed (110) surfaces with 50% coverage of H_3PO molecules. In the upper layers, there are two types of ^{77}Se atoms (•); below the fifth layer (>1 nm), separate calculations on a 17-layer supercell yield a single ^{77}Se environment (▲) with a bulklike ^{77}Se chemical shift [22]. The ^{77}Se MAS NMR spectrum of 5-nm ZnSe nanoparticles along the upper axis is the same as in Fig. 2(c).

of the ^{77}Se MAS signals measured for the ZnSe nanoparticles with mean diameters of 5 and 9 nm: surface electronic perturbations propagate to ^{77}Se atoms in the sixth or seventh layers (i.e., 1–1.2 nm deep) that otherwise have the exact positional ordering of bulk ZnSe within their third or fourth coordination spheres. Furthermore, the isotropic shifts calculated for ^{77}Se atoms in the third layer (-320 ppm) are consistent with the downfield broadening from the bulk signal (-351 ppm, dotted line) observed in the experimental ^{77}Se MAS spectra for the 5- and 9-nm ZnSe nanoparticles [Figs. 2(b) and 2(c)]. Consequently, electronic effects associated with surface relaxation, organic-inorganic interactions, etc., appear to propagate farther than 1 nm into the ZnSe nanoparticles cores. DFT calculations thus show that a major contribution to the broadening of ^{77}Se NMR signals about the bulk ZnSe shift (-351 ppm) in ZnSe nanoparticles is thus accounted for by distributions of electron density that arise as a consequence of the nearby and abrupt termination of the crystal lattice at the exterior nanoparticle surfaces. Contributions from quantum confinement effects and/or local positional disorder of atoms may also be present, although the DFT calculations establish that these appear not to be the dominant influences needed to account for the experimentally observed distributions of isotropic ^{77}Se chemical shifts in the 5-nm ZnSe nanoparticles.

By comparison, similarly calculated isotropic ^{67}Zn chemical shifts ([11], Table S1) show much smaller fluctuations about the signal from bulk ZnSe (<3 ppm below the second layer), compared to the experimental ^{67}Zn linewidths (tens of ppm). Though similar in appearance to those of the respective ^{77}Se MAS spectra [Figs. 2(b)–2(d)], the size-dependent broadenings of the ^{67}Zn spectra [Figs. 2(f)–2(h)] are thus different in nature. In particular, the broader and less resolved spectra are consistent with and accounted for by second-order quadrupolar interactions that are sensitive to perturbations of nearby electric-field gradients at or near the ZnSe nanoparticle surfaces. The broadening of ^{67}Zn and ^{77}Se NMR signals can thus be principally attributed to distributions of local valence electronic environments in otherwise atomically ordered ZnSe nanoparticles.

In conclusion, solid-state ^{77}Se and ^{67}Zn NMR spectra of ZnSe nanoparticles show substantial size-dependent broadening of the NMR resonances that reflects increasing extents of local disorder that propagate >1 nm from the nanoparticle surfaces. Such disorder belies the high degrees of atomic positional order that are independently established by TEM and XRD. DFT calculations of ^{77}Se and ^{67}Zn NMR parameters show that the broad NMR lines can be attributed to perturbations of the electronic density at positionally ordered sites near ZnSe nanoparticle surfaces. Although such ZnSe nanoparticles have generally been labeled ''nanocrystalline'', based on the high degrees of three-dimensional (3D) translational periodic positional ordering of their Zn and Se atoms, they nevertheless exhibit large distributions of local electronic environments. The electronic disorder evidenced here for ZnSe semiconducting nanoparticles is likely to have important implications for the understanding and control of physicochemical properties of a wide range of nanoscale systems for which surface and near-surface effects are expected to play important and in many cases governing roles.

This work was supported in part by the USARO (W911NF-05-1-0085), U.S. NSF (DMR-0233728), U.S.-Israel BSF (2006032). ^{67}Zn NMR spectra were acquired at the NHMFL, Florida State Univ., and DFT calculations conducted through the NCSA, Univ. of Illinois (DMR-070062N). We thank D. Bormann (Orléans), J. Yates (Oxford), and M. J. Gordon (UCSB) for insightful discussions.

*Corresponding author.
bradc@engineering.ucsb.edu

[1] A. P. Alivisatos, Science **271**, 933 (1996).
[2] H. Weller, Curr. Opin. Colloid Interface Sci. **3**, 194 (1998).
[3] G. Hodes, Adv. Mater. **19**, 639 (2007).
[4] W. W. Yu *et al.*, Chem. Mater. **15**, 4300 (2003).
[5] A. B. Panda *et al.*, Langmuir **23**, 765 (2007).
[6] J. T. Hu *et al.*, Science **292**, 2060 (2001).
[7] S. Acharya *et al.*, J. Am. Chem. Soc. **130**, 4594 (2008).
[8] A. Eychmuller, J. Phys. Chem. B **104**, 6514 (2000).
[9] Z. L. Wang, Adv. Mater. **15**, 1497 (2003).
[10] R. L. Penn, J. F. Banfield, Science **281**, 969 (1998).
[11] See EPAPS Document No. E-PRLTAO-103-050940 for materials, characterization, and DFT computational details. For more information on EPAPS, see http://www.aip.org/pubservs/epaps.html.
[12] C. A. Smith *et al.*, Appl. Phys. Lett. **75**, 1688 (1999).
[13] The reflection widths [11] are consistent with coherence lengths (Debye-Scherrer broadening) associated with scattering from nanoparticles with the respective mean sizes observed by TEM, indicating that the contributions of defects, hidden disorder, etc., are probably small.
[14] T. J. Bastow and S. N. Stuart, Phys. Status Solidi B **145**, 719 (1988).
[15] M. G. Berrettini *et al.*, J. Am. Chem. Soc. **126**, 7063 (2004).
[16] C. I. Ratcliffe *et al.*, Phys. Chem. Chem. Phys. **8**, 3510 (2006).
[17] G. Wu, Chem. Phys. Lett. **298**, 375 (1998).
[18] T. J. Bastow, Chem. Phys. Lett. **380**, 516 (2003).
[19] S. J. Clark *et al.*, Z. Kristallogr. **220**, 567 (2005).
[20] J. R. Yates *et al.*, Phys. Rev. B **76**, 024401 (2007).
[21] J. Y. Rempel *et al.*, J. Phys. Chem. B **110**, 18 007 (2006).
[22] The 17-layer ZnSe ZB supercell required the use of a smaller unit cell with 100% coverage of H_3PO molecules and coarser parameters to be computationally feasible [11].